Journal Name

COMMUNICATION

Highly fluorescent water soluble spirobifluorene dye with large Stokes shift: synthesis, characterization and bio-applications

Received 00th January 20xx,
Accepted 00th January 20xx

DOI: 10.1039/x0xx00000x

www.rsc.org/

Friederike Schlüter,[a] Kristina Riehemann,[b] Nermin Seda Kehr,[b] Silvio Quici,[c] Constantin G. Daniliuc[a] and Fabio Rizzo*[a,c]

The first water-soluble spirobifluorene derivative has been synthesized, which exhibits high fluorescence quantum yield and large Stokes shift (>100 nm). Proteins induce change in the emission color, allowing to reach nanomolar detection limit. Cellular uptake and cytotoxicity studies in living cells revealed its biocompatibility, indicating potential application for live cell imaging.

The design of novel fluorescent dyes applicable in biological systems and detectable via high resolution fluorescence microscopy is still challenging.[1] Fluorescent markers for cellular organelles[2] or biomolecules such as DNA[3] or proteins[4] require several features, like large Stokes shift, high molar extinction coefficient (ε) and high quantum yield (QY) to give high brightness (=ε*QY) values in aqueous solution,[5] as well as low cytotoxicity. Although many dyes have been reported so far, combining all aspects in one molecule is still difficult. For example, many highly fluorescent polyaromatic chromophores[6] show small Stokes shifts increasing the difficulty of detection.[7] Moreover, the solubility in pure aqueous solution without adding organic co-solvent is problematic for several efficient dyes, hampering future applications in vivo.[8] The "aggregation induced emission" (AIE) effect offers further options for detection,[9] but the photoluminescence (PL) QY values are low.[10]

Among polyaromatic compounds, spirobifluorene-based molecules attract growing interest due to chemical stability and versatility allowing their use in several technological applications.[11] Typically, a rigid cross-shape spatial conformation is induced by the hybridized sp^3 carbon between the two fluorene halves. So far, the totally absence of reported water soluble spirobifluorene-based molecules precluded the application of spirobifluorene compounds in biological field.

Here, we disclose the synthesis and photophysical properties of the first water soluble spirobifluorene-based fluorescent dye and its interaction with proteins as model system for biological purposes.

Our approach is focused on reducing the quenching caused by aggregation to have high QY while maintaining a large Stokes shift. The dye is based on the spirobifluorene core, which reduces the π–π stacking due to its rigid cross-shape structure, hindering the face-to-face organization between molecules. The phenyl rings bridging the core with amines increase the planarity upon excitation, rising the conjugation between fluorene and amine. As consequence, the emission shifts towards lower energy, without affecting the absorption, resulting in a large Stokes shift.[12] Besides, alkoxy groups in *para*-position of triphenylamines increase the electronic polarizability and sulfonate groups ensure aqueous solubility, by reducing the aromatic packing. This particular design was expected to enable the incorporation of the tetrasodium 2,7-bis(4-(N,N-bis[4-(4-sulfonatobutoxyl)phenyl]amino)phen-1-yl)-9,9'-spirobifluorene (**1**) into hydrophobic pockets of proteins due to the extended aromaticity, acting as highly fluorescent no-covalently bound label with large Stoke shift. The synthesis of dye **1** was carried out in three steps as depicted in Scheme 1.

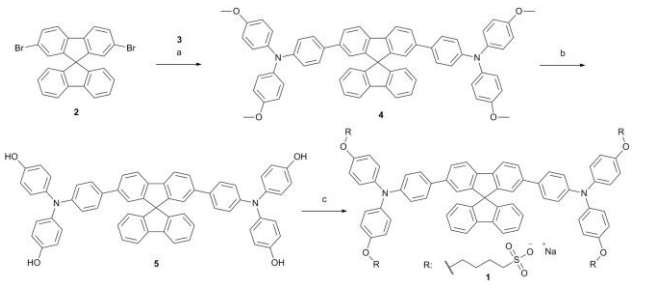

Scheme 1. a) 4-(*N,N*-di(4-methoxyphenyl)amino)phenylboronic pinacol ester (**3**), Na_2CO_3 aq, $Pd(PPh_3)_4$, THF dry, reflux, overnight, 78%; b) BBr_3, CH_2Cl_2 dry, -20 °C to RT, overnight, 88%; c) 1,4-sultone, NaH, DMF dry, RT, overnight, 72%.

[a] *Physikalisches Institut and CeNTech, Westfälische Wilhelms-Universität Münster, Heisenbergstrasse 11, 48149 Münster, Germany.*
[b] *Organisch-Chemisches Institut and CeNTech, Westfälische Wilhelms-Universität Münster, Corrensstrasse 40, 48149 Münster, Germany.*
[c] *Istituto di Scienze e Tecnologie Molecolari (ISTM) and INSTM, Consiglio Nazionale delle Ricerche (CNR), via Golgi 19, 20133 Milano, Italy. E-mail: fabio.rizzo@istm.cnr.it.*

Electronic Supplementary Information (ESI) available: General experimental methods, synthesis of compounds **1**-**5**, photophysical characterization and living cells experiments (fluorescence microscopy and cytotoxicity). See DOI: 10.1039/x0xx00000x

Table 1. Photophysical data of **1**.

solvent [a]	λ_{abs} nm (log ε)	λ_{em} [b] nm (Stokes shift cm^{-1})	ϕ [c] %	τ [d] ns	k_r [e] $*10^8\ s^{-1}$	k_{nr} [e] $*10^8\ s^{-1}$
DMSO	388 (4.85)	510 (6170)	69	3.35 (98%); 0.14 (2%)	20.6	9.2
DMF	385 (4.80)	505 (6170)	67	3.23 (99%); 0.11 (1%)	20.7	10.2
MeOH	379 (4.88)	487 (5850)	64	2.74 (93%); 0.08 (7%)	23.3	13.1
H_2O	378 (4.71)	480 (5620)	50	4.23 (77%); 0.90 (15%); 0.09 (8%)	11.8	11.8
PBS with BSA [f]	378	461 (4760)	87	3.55 (72%); 1.55 (25%); 0.15 (3%)	24.5	3.7
Triton X-100	385	461 (4280)	88	3.17 (66%); 1.22 (30%); 0.21 (4%)	27.8	3.8

[a]Measurements performed using a concentration of 10^{-6} M. [b]Recorded exciting at 378 nm. [c]Calculated using integrated sphere. Value ±2. [d]Value ±0.01 ns. [e]From $k_r=QY/\tau$ and $k_{nr}=(1-QY)/\tau$ by using τ main component. [f] in presence of 0.6 μM BSA.

The first step of the synthesis was Suzuki coupling between 2,7-dibromo-9,9'-spirobifluorene (**2**) core and 4-(*N*,*N*-di(4-methoxyphenyl)amino)phenylboronic pinacol ester (**3**). The deprotection of intermediate **4** by treatment with boron tribromide (BBr_3), followed by the alkylation of **5** with 1,4-butansultone in the presence of sodium hydride allowed to obtain the desired product. The pure **1** was easily obtained by precipitation, as confirmed by NMR and high-resolution mass analysis (see SI).

Pure water, aqueous phosphate-buffer (PBS) as well the organic solvents dimethylformamide (DMF), dimethylsulfoxide (DMSO) and methanol (MeOH) effectively solubilize **1** and the photophysical data are summarized in Table 1.

Noteworthy, the four sulfonate groups give excellent solubility of the dye in water (1.56×10^{-2} mol/L).

The absorption spectrum shows two main bands in the UV region with maxima at 280 nm and around 380 nm (Figure 1a). In agreement with very similar compounds,[12] we can attribute the low energy band to π–π* transition of the conjugated backbone.

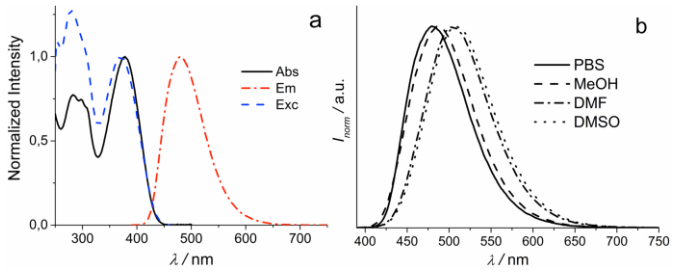

Figure 1. a) Normalized absorption, PL (λ_{exc} = 378 nm) and excitation (λ_{em} = 487 nm) spectra of **1** (3 μM) in PBS; b) Normalized PL in different solvents.

The dye emits intense blue-green light depending on the solvent, even though the lack of strong acceptor groups causes slight sensitivity towards the solvent polarity (Figure 1b). Notably, large Stokes shifts over 100 nm were measured in all mentioned solvents. The QY is slightly affected by the nature of the solvent, and remains high even in H_2O. Remarkably, the brightness of **1** in aqueous solution is higher than commercial dyes used as cell markers like DAPI.[2c,13] Radiative decays in organic solvents are almost monoexponential, with a dominant slow component τ_1 around 3 ns.

Interestingly, protic solvents induce blue-shifted absorption and emission spectra compared to DMSO, albeit the polarity increases. This behavior arises reasonably from hydrogen bonding formation, which reduce the conjugation length in the excited state, thus increasing the energy of the system **1**–solvent. As observable effect, the PL is blue shifted.[7] The crystal structure of **4**[14] (Figures S1 and S2) and the absorption measured at different temperatures clarify the decrease of the ε value in H_2O compared to organic solvents. The lower energy absorption band enhances without shift by increasing the temperature, suggesting the presence of undefined aggregates (Figure S3). Although the rigid molecular core of **1** hampers the π–π stacking, unspecific aggregation could occurred due to the extended hydrophobic core and hydrogen bonding, as suggested by the crystal structure of **4**. In fact, the π–π stacking is absent, while the packing is driven by *CH*–π and *O*–*H* interactions, with an interesting and crucial different binding behavior of the oxygen atoms (Figure S2 and Table S1). This interpretation clarifies also the decrease of QY in H_2O, supported by the multiexponential radiative decay. Moreover, higher concentrations are not affecting the PL band, while a small red shift of the emission at high dilution was observed (Figure S4). A similar behavior was also observed at high viscosity by measuring **1** in MeOH/glycerol mixtures (Table S2 and Figure S5).

We further investigated the influence of the pH on the fluorescent properties of **1**. The emission intensity is stable in basic and neutral condition, while begins to decrease between pH 6 and 4 and at low pH the emission is almost completely quenched (Figure S6).

The excellent water solubility, the high brightness in aqueous solution and the stability of the PL intensity along the biological pH range are positive features for the use of the spirobifluorene-based dye in bio-applications.

The suitability of **1** as protein marker was assessed by using bovine serum albumin (BSA) as model protein. Adding BSA to **1** has no remarkable effect on the π–π* absorption band, while the enhancement of the peak at 280 nm corresponds to the protein absorption (Figure S7). In contrast, the emission changed instantaneously, leading to a clear color variation from green to blue already detectable with naked eyes under UV lamp (Figure 2). The PL spectrum shows hypsochromic shift and the shrinkage of full-width at half maximum (fwhm, Table S3) in presence of BSA, jointly with increasing intensity and QY.

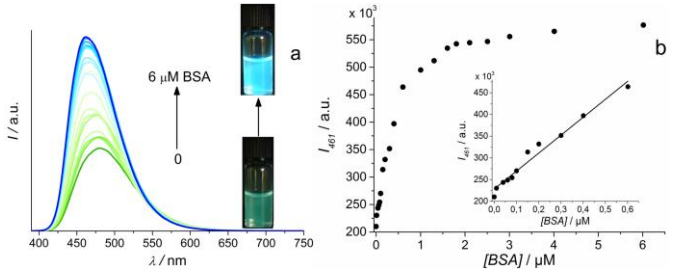

Figure 2. Titration experiment of **1** (3 μM) with BSA (PBS, pH 7.2): a) PL (λ_{exc} = 378 nm), b) intensity vs. BSA concentration. The inset shows the fit in the linear range.

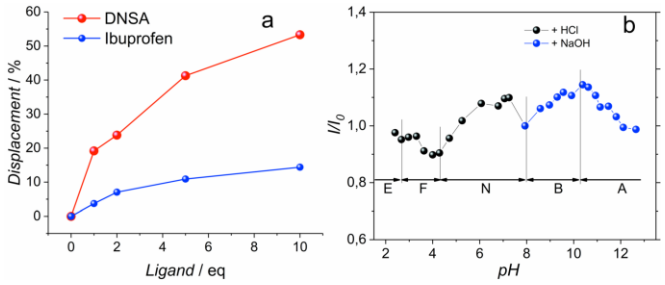

Figure 3. a) Displacement in presence of dansylamide or Ibuprofen, b) variation of PL intensity of **1**:BSA vs. pH in relationship with BSA conformers. I_0 is the intensity at neutral pH.

Titration experiments were performed to evaluate the sensitivity of **1**. The PL intensity rises linearly with the BSA concentration in a wide range up to 600 nM, which became almost constant after 2 μM. The calculated limit of detection (LOD) (See SI) was 7.3 nM in the linear range, proving to be more sensitive than probes based on AIE phenomenon[15] and other techniques used for detection of BSA in real sample like high-performance liquid chromatography,[16] again indicating the high sensitivity of **1** towards BSA.

The overlap between the absorption of **1** and the emission of BSA suggests the presence of intermolecular resonance energy transfer (RET).[7] However, the calculation of the binding constant throughout the quenching of the BSA emission at different concentration of **1** (Stern-Volmer analysis,[7] Figure S8) gives too large value. Thus the binding constant K = 2.62 × 10^6 M^{-1} was calculated from fluorescence data through the Hill equation and confirmed by other fitting methods (Figure S9), indicating high affinity between BSA and **1**. From Hill analysis we calculated also the stoichiometry of the complex (n = 1.2), resulting in a 1:1 ratio of dye:BSA, as confirmed by the linear fit in the Benesi-Hildebrand analysis (Figure S9c).

To verify the dye specificity towards serum albumin, we tested **1** in presence of other proteins (protamine, horseradish peroxidase HRP, pepsin) (Figure S10). The PL reveals that only BSA induces highly intense blue shifted emission, while pepsin slightly increases the intensity without shift, and protamine and HRP causes lower blue shifted PL.

It is well known the presence of two sites in BSA (Sudlow's site I and site II) in which organic dyes are bound depending on the nature of the interaction with BSA (mainly hydrophobic for site I and electrostatic for site II).[17] We investigated the variation of PL intensity of the system **1**:BSA by addition of known site-marker compounds (dansylamide DNSA for site I and Ibuprofen for site II)[18] to determine the binding site of **1**. As depicted in Figure 3a, the ligand displacement obtained for DNSA is higher than for Ibuprofen, indicating thereby the possibility to bind both sites, with preference to site I. The hydrophobicity of site I justifies the blue shift of the emission due to the lower polarity in the local environment. However, the displacement observed also with Ibuprofen confirms the presence of electrostatic interactions between the two species.

We measured the PL of the **1**:BSA system at different pH to investigate the role of the electrostatic attraction. The effect of pH on binary system appears very different compared to the free dye (see Figure S6 and S11). Indeed, the high PL intensity in the pH range 2–13 indicates strong interaction and high stability between dye and protein. Very interestingly, the trend of the PL maximum is associated with the change of BSA conformation (Figure 3b), as effect of the predominance of one of two kind of interactions (electrostatic at low pH and hydrophobic at basic pH). Then, **1** is influenced by the variation of the net charge and by the conformers of the protein.[19] Besides, we verified by CD spectroscopy that the denaturation of BSA is not caused by **1** (Figure S12).

Due to the micellar behavior of BSA at neutral pH, the study of **1** in different surfactants allowed us to explore its local environment (Figure S13, Table S3). Compared to pure water, the decrease of hydrogen bonds formation leads to an increase in PL intensity independently on the nature of surfactant (anionic, cationic or nonionic). The PL is not notably shifted in sodium dodecyl sulfate (SDS), while the bathochromic shift in cationic cetyltrimethylammonium bromide (CTAB) indicates a locally increase of polarity. Interestingly, the highest enhancement of the emission occur in neutral surfactants Tween 20 and Triton X-100 (TX). However, only in TX a blue shifted PL with smaller fwhm like in the presence of BSA was observed, suggesting a lower polarity in the microenvironment due to the aromatic core of the TX.[20] Besides, lifetime data suggest that the aromatic rings in TX hamper the rotational movement of phenyl rings in **1**, reducing the non-radiative deactivation path. In fact, the longest component is very similar to aprotic solvents, and the non-radiative rate k_{nr} dropped by a factor of 3. Due to the similarity of lifetime data and PL profiles (Figure S13), we expect comparable local environment in TX and BSA.

We tested the ability of **1** as a cell marker using healthy primary human Fibroblast, Human Umbilical Vein Endothelial cells (HUVEC) and primary Macrophages from the peripheral blood. Noteworthy, the dye doesn't need addition of organic co-solvent to be solubilized. Fluorescence microscopy images recorded at different concentrations (from 1 μM to 50 μM) showed the uptake of **1** by living cells and an accumulation in vesicle-like structures within the cytoplasm (Figure 4 and S14).

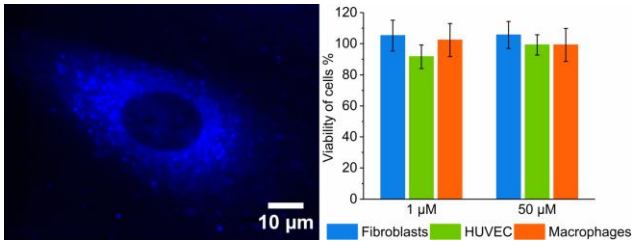

Figure 4. Fluorescence microscopy image (left) of living Fibroblast cells incubated with **1** (1 µM in PBS). Cell viability XTT assay (right) of primary human fibroblast, HUVEC and macrophages incubated with **1** at different concentration.

In addition, the XTT assay test proved that **1** has no cytotoxic effects even at high concentration, thus indicating 1 as an ideal reagent for live cell imaging of different types of primary cells.

In conclusion, the design of the first water soluble spirobifluorene-based molecule **1** allowed combining a large Stokes shift and high QY in aqueous solution as well in organic solvents. The presence of BSA induced a blue shifted emission with increased QY, resulting in a nanomolar detection limit for BSA in a no covalent labelled analysis. By using known site-marker molecules, we observed the simultaneous presence of hydrophobic and electrostatic interactions in the **1**:BSA complex. Interestingly, the variation of pH suggests an enhancement of one interaction over the other, resulting in a strong binding and intense emission in the whole pH range. Besides, at neutral pH the local polarity of **1**:BSA system is analogous to micelles formed by Triton X-100. The interaction between aromatic rings in the supramolecular species BSA–**1** reduces the deactivation pathways and changes the polarity in the local surroundings of the dye, inducing blue-shifted PL. Finally, **1** demonstrates that spirobifluorene derivatives may provide useful tools for the imaging of biological pathways in living cells due to their excellent solubility in aqueous solution combined with high brightness and very low cytotoxicity. Spirobifluorene-based molecules emitting at lower energy and able to address specific organelle are actually under investigation in our laboratories.

F.R. thanks Prof. B. J. Ravoo for access to his laboratories and fruitful discussion, Prof. Dr. G. Wilde and Priv.-Doz. Dr. C. A. Strassert for the kind use of their instruments, Prof. G. Fernandez for fruitful discussion and Deutscher Akademischer Austauschdienst (DAAD) for fellowship. Judith Schmidt and Jana Salich are acknowledged for the excellent technical support.

Notes and references

1 (*a*) M. Fernández-Suárez and A. Y. Ting, *Nat. Rev. Mol. Cell. Biol.,* 2008, **9**, 929; (*b*) H. Schill, S. Nizamov, F. Bottanelli, J. Bierwagen, V. N. Belov and S. W. Hell, *Chem. Eur. J.,* 2013, **19**, 16556; (*c*) C. Eggeling and S. W. Hell, *STED Fluorescence Nanoscopy, Springer Ser. In Fluorescence,* Eds.: P. Tinnefeld, C. Eggeling, S. W. Hell, Springer, Berlin-Heidelberg, 2015, pp. 4-25; (*d*) M. V. Sednev, V. N. Belov and S. W. Hell, *Methods Appl. Fluoresc.,* 2015, **3**, 042004.

2 (*a*) B. N. G. Giepmans, S. A. Adams, M. H. Ellisman and R. Y. Tsien, *Science*, 2006, **312**, 217; (*b*) W. Xu, Z. Zeng, J.-H. Jiang, Y.-T. Chang and L. Yuan, *Angew. Chem. Int. Ed.,* 2016, **55**, 13658; (*c*) L. D. Lavis and R. T. Raines, *ACS Chem. Biol.,* 2008, **3**, 142.

3 Recent examples: (*a*) L. Hahn, N. J. Buurma and L. H. Gade, *Chem. Eur. J.,* 2016, **22**, 6314; (*b*) J. Jeffet, A. Kobo, T. Su, A. Grunwald, O. Green, A. N. Nilsson, E. Eisenberg, T. Ambjörnsson, F. Westerlund, E. Weinhold, D. Shabat, P. K. Purohit and Y. Ebenstein, *ACS Nano*, 2016, **10**, 9823.

4 Recent examples: (*a*) T. Sarkar, K. Selvakumar, L. Motiei and D. Margulies, *Nat. Commun.,* 2016, **7**:11374, doi:10.1038/ncomms11374; (*b*) L. Unger-Angel, B. Rout, T. Ilani, M. Eisenstein, L. Motiei and D. Margulies, *Chem. Sci.*, 2015, **6**, 5419.

5 (*a*) H. Kobayashi, M. Ogawa, R. Alford, P. L. Choyke and Y. Urano, *Chem. Rev.,* 2010, **110**, 2620; (*b*) S. Nizamov, M. V. Sednev, M. L. Bossi, E. Hebisch, H. Frauendorf, S. E. Lehnart, V. N. Belov and S. W. Hell, *Chem. Eur. J.,* 2016, **22**, 11631.

6 (*a*) A. Martínez-Peragón, D. Miguel, R. Jurado, J. Justicia, J. M. Álvarez-Pez, J. M. Cuerva and L. Crovetto*, Chem. Eur. J.,* 2014, **20**, 447; (*b*) M. Beija, C. A. M. Afonso and J. M. G. Martinho, *Chem. Soc. Rev.*, 2009, **38**, 2410; (*c*) A. N. Butkevich, G. Y. Mitronova, S. C. Sidenstein, J. L. Klocke, D. Kamin, D. N. H. Meineke, E. D'Este, P.-T. Kraemer, J. G. Danzl, V. N. Belov and S. W. Hell, *Angew. Chem. Int. Ed.,* 2016, **55**, 3290; (*d*) A. Poirel, P. Retailleau, A. De Nicola and R. Ziessel, *Chem. Eur. J.,* 2014, **20**, 1252; (*e*) S. Kaloyanova, Y. Zagranyarski, S. Ritz, M. Hanulová, K. Koynov, A. Vonderheit, K. Müllen and K. Peneva, *J. Am. Chem. Soc.,* 2016, **138**, 2881; (*f*) L. Hahn. S. Öz, H. Wadepohl and L. H. Gade, *Chem. Commun.,* 2014, **50**, 4941; (*g*) E. Heyer, P. Lory, J. Leprince, M. Moreau, A. Romieu, M. Guardigli, A. Roda and R. Ziessel, *Angew. Chem. Int. Ed.,* 2015, **54**, 2995.

7 J. R. Lakowicz, *Principles of Fluorescence Spectroscopy*, 3rd ed., Kluwer Academic/Plenum Publishers, New York, 2006.

8 Y. Liu, J. Zhou, L. Wang, X. Hu, X. Liu, M. Liu, Z. Cao, D. Shangguan and W. Tan*, J. Am. Chem. Soc.,* 2016, **138**, 12368.

9 (*a*) J. Mei, N. L. C. Leung, R. T. K. Kwok, J. W. Y. Lam and B. Z. Tang, *Chem. Rev.,* 2015, **115**, 11718; (*b*) H. Qian, M. E. Cousins, E. H. Horak, A. Wakefield, M. D. Liptak and I. Aprahamian, *Nat. Chem.,* 2017, **9**, 83.

10 H. Frisch, D. Spitzer, M. Haase, T. Basche, J. Voskuhl and P. Besenius, *Org. Biomol. Chem.,* 2016, **14**, 5574.

11 T. P. I. Saragi, T. Spehr, A. Siebert, T. Fuhrmann-Lieker and J. Salbeck, *Chem. Rev.,* 2007, **107**, 1011.

12 (*a*) F. Polo, F. Rizzo, M. Veiga-Gutierrez, L. De Cola and S. Quici, *J. Am. Chem. Soc.,* 2012, **134**, 15402; (*b*) F. Rizzo, F. Polo, G. Bottaro, S. Fantacci, S. Antonello, L. Armelao, S. Quici and F. Maran, *J. Am. Chem. Soc.,* 2017, **139**, 2060; (c) T. Komino, H. Nomura, M. Yahiro, K. Endo, and C. Adachi, *J. Phys. Chem. C* 2011, **115**, 19890.

13 D. R. G. Ditter, A. S. Brown, J. D. Baker and J. N. Wilson, *Org. Biomol. Chem.,* 2015, **13**, 9477.

14 CCDC 1565161 (**4**) contains the supplementary crystallographic data for this paper. These data can be obtained free of charge from The Cambridge Crystallographic Data Centre via www.ccdc.cam.ac.uk/data_request/cif.

15 H. Tong, Y. Hong, Y. Dong, M. Häussler, Z. Li, J. W. Y. Lam, Y. Dong, H. H.-Y. Sung, I. D. Williams and B. Z. Tong, *J. Phys. Chem. B,* 2007, **111**, 11817.

16 A. Hesse and M. G. Weller, *J. Amino Acids*, 2016, Article ID 7374316, doi: 10.1155/2016/7374316.

17 T. Peters, Jr. *All about albumin*, 1st ed., Academic Press, US, 1995.

18 R. K. Pandey, S. Constantine, T. Tsuchida, G. Zheng, C. J. Medforth, M. Aoudia, A. N. Kozyrev, M. A. J. Rodgers, H. Kato, K. M. Smith and T. J. Dougherty, *J. Med. Chem.* 1997, **40**, 2770.

19 Z. Yang, J. Cao, Y. He, J. H. Yang, T. Kim, X. Peng and J. S. Kim, *Chem. Soc. Rev.,* 2014, **43**, 4563.

20 (*a*) A. Nag and K. Bhattacharyya, *J. Photochem. Photobiol. A Chem.,* 1989, **47**, 97; (*b*) G. Saroja and A. Samanta, *Chem. Phys. Lett.,* 1995, **246**, 506.

